

RESEARCH

Open Access



Downstream impacts of dam breach using HEC-RAS: a case of Budhigandaki concrete arch dam in central Nepal

Anu Awal¹, Utsav Bhattarai², Vishnu Prasad Pandey³ and Pawan Kumar Bhattarai^{4*}

Abstract

Studies on concrete dam breach are limited compared to earthen and other types of dams. With an increase in the construction of concrete dams, particularly in the developing world, it is imperative to have a better understanding of the dam breach phenomena and the identification of the most influential breach parameters. This study aims to contribute to this gap by taking the case of the concrete arch dam proposed for the 1200 MW Budhigandaki Hydropower Project located in central Nepal. This study carries special significance for Nepal, primarily because of the increasing number of under construction and proposed large dams for water resources development in the country. We carry out dam breach analysis of the Budhigandaki dam using HEC-RAS 2D model to calculate the flood discharge peaks, time to peak, water surface elevation and the extent of inundation for two scenarios (with and without probable maximum flood) to estimate the damage on four downstream settlements. We carry out sensitivity analysis of the breach parameters on the flood magnitudes and severity. Results show that all the study locations lie in the high flood hazard zone. Flood peaks can reach as high as $286,000 \text{ m}^3\text{s}^{-1}$ to $511,000 \text{ m}^3\text{s}^{-1}$ in the considered settlements. The time to peak ranges from 11.3 to 17 h after the breach at these locations. We estimate that if a breach should happen, it would most likely inundate around 150,000 buildings, impact nearly 672,000 lives and flood 3,500 km of road downstream. Furthermore, dam breach elevation is found to be the most sensitive parameter to downstream floods. Hence, rather than structural measures, it is recommended that non-structural measures are implemented for minimizing the impacts of flood disasters at the study locations. The findings could be a useful reference for future dam projects in Nepal and other areas with similar hydrological and topographical conditions.

Keywords Dam breach, HEC-RAS, Downstream impacts, Sensitivity analysis, Budhigandaki dam

*Correspondence:

Pawan Kumar Bhattarai

pawan.bhattarai@ioe.edu.np

¹Nepal Engineering College, Pokhara University, Bhaktapur, Nepal

²Institute for Life Sciences and the Environment, University of Southern Queensland, Toowoomba, Australia

³Centre for Water Resources Studies, Institute of Engineering, Tribhuvan University, Lalitpur, Nepal

⁴Department of Civil Engineering, Pulchowk Campus, Institute of Engineering, Tribhuvan University, Lalitpur, Nepal



© The Author(s) 2024. **Open Access** This article is licensed under a Creative Commons Attribution-NonCommercial-NoDerivatives 4.0 International License, which permits any non-commercial use, sharing, distribution and reproduction in any medium or format, as long as you give appropriate credit to the original author(s) and the source, provide a link to the Creative Commons licence, and indicate if you modified the licensed material. You do not have permission under this licence to share adapted material derived from this article or parts of it. The images or other third party material in this article are included in the article's Creative Commons licence, unless indicated otherwise in a credit line to the material. If material is not included in the article's Creative Commons licence and your intended use is not permitted by statutory regulation or exceeds the permitted use, you will need to obtain permission directly from the copyright holder. To view a copy of this licence, visit <http://creativecommons.org/licenses/by-nc-nd/4.0/>.

Introduction

Dams are storage structures providing beneficial functions such as flood control and water supply for different types of users (for example, domestic water supply, hydropower, irrigation, recreation and water transport). The construction of large dams along with generation of electricity started during the industrial revolution in Europe and America. The early 1900s ushered in an era of “big dam” building in America mostly for hydropower generation as demands for electricity increased, the Hoover Dam being regarded as an engineering marvel. The Asian region includes some of the largest dams in the world today such as Tarbela Dam and Mangla Dam in Pakistan, Nurek Dam in Tajikistan, San Rogue Dam in Phillipines and Three Gorges Dam in China, mostly for hydropower generation.

Despite the benefits, failure of dams can cause tremendous losses by generation of unforeseen flood magnitudes in downstream areas. Unfortunately, the history of dams has been studded with disasters of various types, sometimes of great magnitude, with loss of human lives and destruction of property and infrastructure (Aureli et al. 2021). USACE (2018) lists causes of dam breach as earthquakes, landslides, extreme storms, piping, equipment malfunction, structural damage, foundation failure, and sabotage. Regardless of the reason, almost all failures begin with a breach formation.

Basically, breach is defined as the opening formed in the dam body that leads the dam to fail and this phenomenon causes the stored water behind the dam to propagate rapidly downstream (Dincergok 2007). Despite piping or overtopping being the main modes of dam failure, the actual mechanics are still not completely understood for either earthen or concrete dams (USACE 2018). Past dam-failure disasters have shown that the majority of dams that have failed are earthen (74 dam breaks out of 7812 earthen dams) and the highest percentage of failure of rockfill dams (17 dam breaks out of 200 rockfill dams) (Fang et al. 2017). The world’s worst dam disaster happened in China in 1975 when the Banqiao and Shimantan dams failed killing about 171,000 people while 11 million lost their homes (Vincent et al. 2020). In 1979, the 25 m high Machu Dam in India, which stored 100 million m³, failed after several hours of over-topping causing about 10,000 deaths, 150,000 people were displaced, and 10,000 habitations were destroyed (Lempérière 2017). A recent case of the failure of the Rishiganga dam in Uttarakhand (India) in 2021 due to glacier avalanche caused more than 200 deaths and severely damaged infrastructure (Shugar et al. 2021). Similarly, failure of the Edenville dam followed by the Sanford dam downstream on the same day in 2020 due to heavy rain in Michigan USA (Independent Forensic Team 2022), and failure of the Spencer Dam in Nebraska USA in 2019 due to ice run (Ettema et al. 2021),

demonstrate the devastation that dam breaches can lead to. Thus, identification of the vulnerable areas and being aware of the likely damages are key for minimization of the adverse impacts of dam breach.

Dam breach analysis involves three key sequential steps: predicting the reservoir outflow hydrograph, determining dam breach parameters, and routing the hydrograph downstream. Essentially, the breach flood hydrograph depends on the prediction of breach geometry and breach formation time (Basheer et al. 2017). There have been many studies on dam breach analysis around the world from the 1980’s (Leng et al. 2023; Singh and Snorrason 1984; USACE 2024). Dam breach analysis is generally carried out by either numerical/computer models or scaled-down physical models. The United States Department of Interior (1988), recommends estimating a reasonable maximum breach discharge using four principal methods:

Physically Based Methods: Using erosion models based on principles of hydraulics, sediment transport and soil mechanics, development of breach and resulting breach outflow are estimated;

Parametric Models: Time to failure and ultimate breach geometry are assessed utilizing case studies; breach growth is simulated as a time-dependent linear process and breach outflows are computed using principles of hydraulics;

Predictor Equations: Using data of case studies, peak discharge is estimated from empirical equations and a reasonable shape of outflow hydrograph is assumed; and.

Comparative Analysis: Breach parameters are determined by comparison of dam under consideration and a dam that failed.

There are far fewer studies on the failures of concrete dams compared to earthen dams, especially due to breaches which leads to difficulty in determining the concrete dam breach parameters (Fang et al. 2017). Moreover, a study of well documented dam-failure cases showed that empirical formulas provide results closer to reality (Fang et al. 2017). For instance, Froehlich(1995) developed a prediction equation for the average breach width based on 63 cases of embankment-dam failures and an equation for the breach-formation time based on 21 cases. Focusing on earthen dams has been driven by their historical prevalence, cost-effectiveness, and adaptability. However, studying concrete arch dams is crucial for advancing engineering practices, improving safety and efficiency in dam construction, supporting hydro-electric power generation, addressing environmental impacts, and preserving significant cultural landmarks. Many federal agencies such as FERC (1993), Office of the State Engineer(2020) and USACE (2014) have published

guidelines recommending possible ranges of values for breach width, side slopes, and development time for different types of dams. This study aims to investigate the breach characteristics of concrete arch dams, an area with limited existing literature. Several dam breach analysis studies have been carried out in Nepal such as in Kulekhani dam using HEC-RAS (Pandey et al. 2023), Kaligandaki landslide dam using BREACH (Bricker et al. 2017), Koshi high dam using HEC-RAS (Gyawali, D.R. and Devkota, 2015), among others. However, no sensitivity analysis of dam breach parameters has been carried out for the afore-mentioned studies.

The proposed Budhigandaki dam located in the trans-boundary Budhigandaki Basin, spread over southern China and central Nepal, is taken as a case. The Government of Nepal (GoN) has prioritized hydropower generation as the backbone of economic development to attain the goals to raise the country's status to middle income country level by 2030 (Government of Nepal 2020). As a result, there are currently more than 9 planned and proposed large hydropower dam projects by the state (Nepal Electricity Authority 2022). The Budhigandaki Hydropower Project (BGHPP) could be the largest storage project of Nepal, if constructed, which could lead to catastrophic damages downstream in the event of a breach.

Hence, the overarching objective of this study is to assess the flood impacts of the Budhigandaki Dam on the downstream settlements due to possible dam breach scenarios. Specifically, this study intends to quantify the peak discharge, time to peak, and the water surface elevation at the downstream locations due to a dam-breach flood. Further, sensitivity analysis of five different dam breach parameters is conducted to acquire information about extent of influence of each parameter on the dam breach. The analysis is carried out in the widely-used hydraulic model Hydrologic Engineering Center's - River Analysis System (HEC-RAS) developed by the United States Army Corps of Engineers (USACE). Furthermore, zoning of the downstream settlement areas in Geographic Information System (GIS) based on flood severity provides meaningful information to the project developers as well as planners in the impacted areas.

Materials and methods

Study area

The Budhigandaki Hydropower Project (BGHPP) is a 1200 MW storage type proposed project of Nepal located approximately 2 km upstream of the confluence of Budhigandaki River with Trishuli River as shown in Fig. 1. The Budhigandaki Dam is a 263 m high double curvature concrete arch dam with a reservoir volume of 4.5 billion cubic meters (BCM), out of which the active storage is 2.2 BCM. The dam crest length is 737.4 m and the reservoir Full Supply Level (FSL) is at 540 m above sea level

(masl) (Budhigandaki Development Committee, 14a). There are some major settlement areas nearly 110 km downstream which are susceptible to danger in case of dam breach. For this study, four major towns namely, Narayangarh, Baraghare, Divyanagar and Meghauri, have been assessed. Moreover, future risk of impact from the dam failure can be expected to increase as increased in population growth due to improved job opportunities and other economic activities in the area because of the construction of the dam. Therefore, the Budhigandaki Dam has been taken as a case in this study to assess the flooding impacts of the dam on the downstream areas through simulation of a hypothetical dam failure.

Methodology

Dam breach analysis of the Budhigandaki dam has been carried out in HEC-RAS using unsteady flow simulation with terrain and land cover as the geometric input data. The upstream boundary condition is the probable maximum flood (PMF) hydrograph which has been generated using an empirical method while the downstream boundary condition is normal depth. Two dam failure scenarios, namely, dam breach at reservoir full condition with PMF (Scenario I: base case) and dam breach at reservoir full condition without PMF (Scenario II), have been modelled in the study. Outputs of the simulation are used for creating flood inundation maps, flood hazard vulnerability maps and flood arrival time maps corresponding to the different scenarios. Sensitivity analysis of the dam breach parameters is also carried out to assess their impacts on the flood conditions downstream of the dam. Figure 2 summarizes the overall research methodology.

Data

The spatial inputs required to model the dam breach are digital elevation model (DEM), land cover and Manning's roughness coefficient. Rainfall and discharge are needed for generation of inflow hydrograph as upstream boundary condition to the model. In addition, infrastructure data of the downstream area is required for estimating the impacts of floods. Details of the required data and their sources are presented in Table 1.

PMP and PMF

The probable maximum precipitation (PMP) is the theoretical maximum precipitation for a given duration under current meteorological conditions (World Meteorological Organization 2009). Daily maximum rainfall data of 13 surrounding stations from 1972 to 2014 has been used for the calculation of PMP. The 1-day PMP for all the stations was calculated using Hershfield formula (Hershfield 1965) given in Eq. (1) :

$$PMP = M + K.S \quad (1)$$

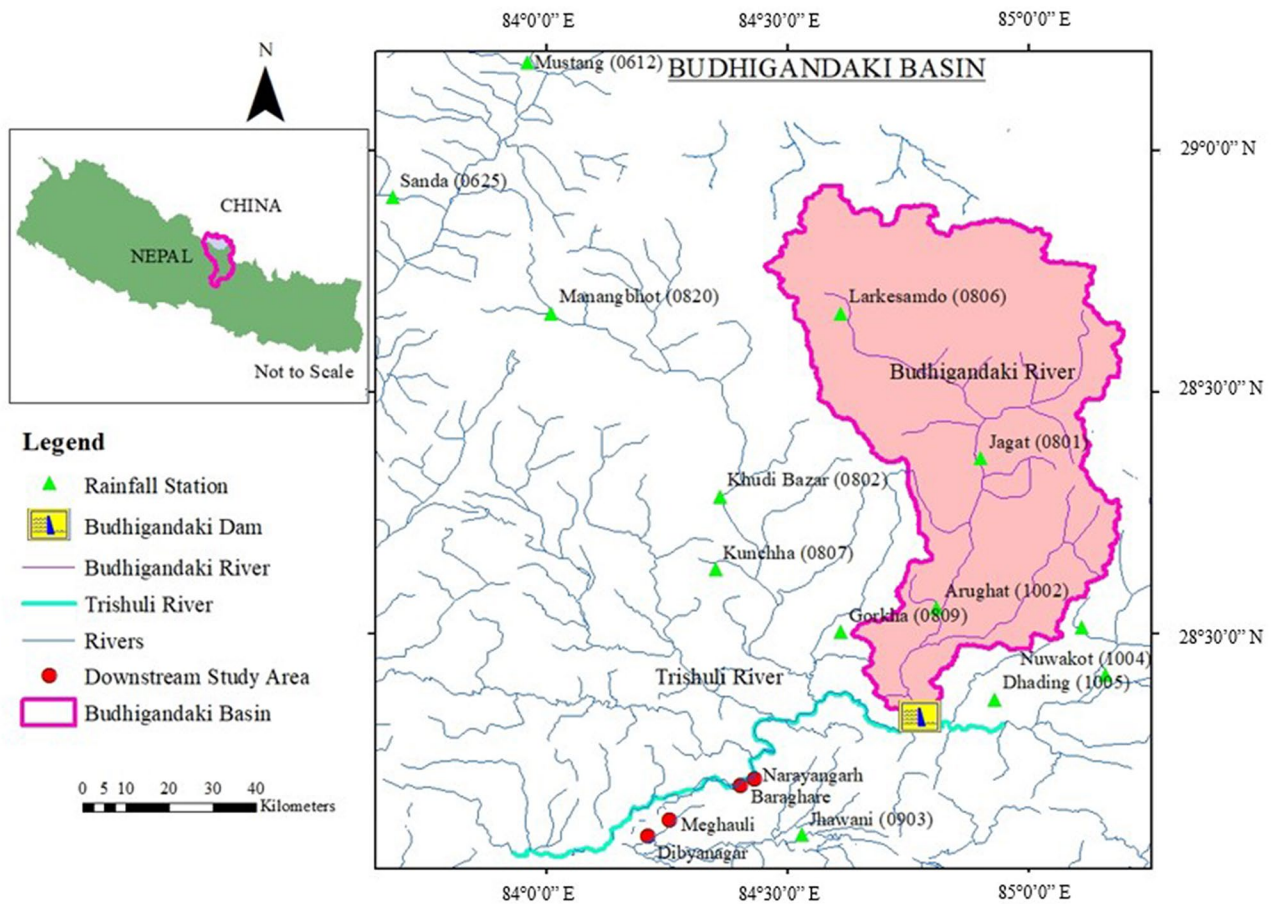


Fig. 1 Location of Budhigandaki dam and downstream settlement areas

Where, *PMP*= Probable maximum precipitation.

M=mean of maximum daily rainfall sample *S*=Standard deviation.

K=Frequency factor= 15 (Hershfield 1965).

The calculated 1-day PMP of the point stations was further interpolated using Thiessen Polygon, Kriging, Spline and Inverse Distance Weighing (IDW) methods in GIS to compute the 1-day PMP for the Budhigandaki Basin. In order to model a worst-case scenario, the maximum value of the PMP among these methods was chosen for generating the PMF hydrograph.

Probable Maximum Flood (PMF) is theoretically the flood resulting from a combination of the most severe meteorological and hydrologic conditions that could conceivably occur in a given area (FERC 2001). HEC-RAS requires a flood hydrograph to be provided as input for the unsteady flow analysis in the dam breach model. Therefore, a synthetic unit hydrograph was developed using Snyder’s Method (American Geophysical Union 1938) using the following equations (Eq. (2) to Eq. (7) which was then transposed to generate a direct runoff hydrograph of PMF.

Mathematically,

$$T_{lag} = C_t(L * L_{ca})^{0.3} \tag{2}$$

$$T_d = \frac{T_{lag}}{5.5} \tag{3}$$

$$q_p = \frac{640 * A * C_p}{T_{lag}} \tag{4}$$

$$T_b = 3 + \frac{T_{lag}}{8} \tag{5}$$

$$W_{50} = 770 * \left(\frac{q_p}{A}\right)^{-1.08} \tag{6}$$

$$W_{75} = 440 * \left(\frac{q_p}{A}\right)^{-1.08} \tag{7}$$

Dam breach analysis

Dam breach analysis of the Budhigandaki dam has been carried out in HEC-RAS model under two-dimensional dynamic (unsteady-flow) mode. Hypothetical breach of the dam and its propagation downstream has been

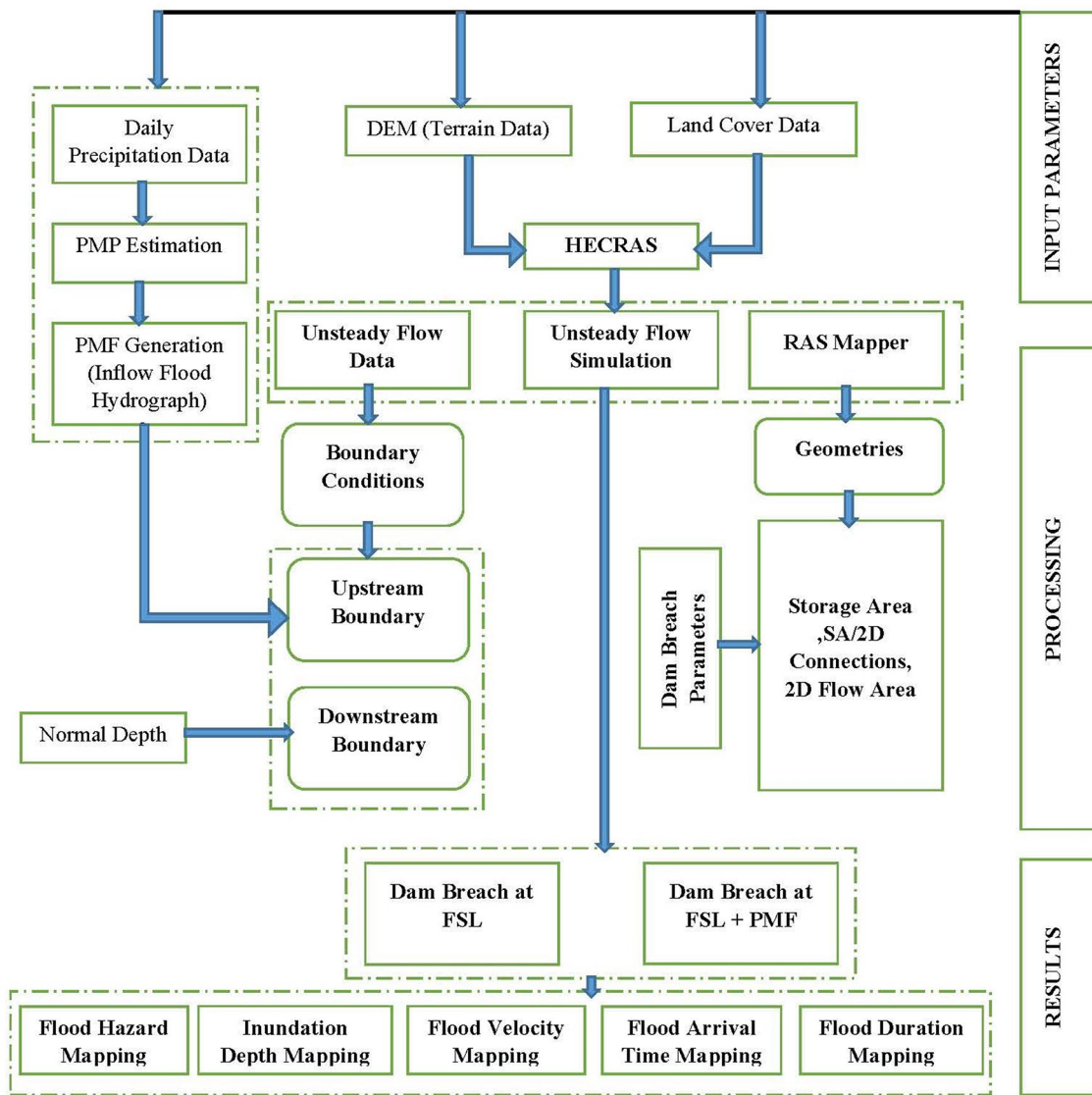


Fig. 2 Overall research methodology of this study. DEM: Digital Elevation Model, PMP: Probable Maximum Precipitation, PMF: Probable Maximum Flood, SA: Storage Area, 2D: Two Dimensional, FSL: Full Supply Level

modelled using 2D Diffusion wave equations (Eq. (8) to Eq. (10)).

$$\frac{\partial \zeta}{\partial t} + \frac{\partial p}{\partial x} + \frac{\partial q}{\partial y} = 0 \tag{8}$$

$$\frac{\partial p}{\partial t} + \frac{\partial}{\partial x} \left(\frac{p^2}{h} \right) + \frac{\partial}{\partial y} \left(\frac{pq}{h} \right) = - \frac{n^2 pg \sqrt{p^2 + q^2}}{h^2} - gh \frac{\partial \zeta}{\partial x} + pf + \frac{\partial}{\rho \partial x} (h\tau_{xx}) + \frac{\partial}{\rho \partial y} (h\tau_{xy}) \tag{9}$$

$$\frac{\partial q}{\partial t} + \frac{\partial}{\partial x} \left(\frac{q^2}{h} \right) + \frac{\partial}{\partial y} \left(\frac{pq}{h} \right) = - \frac{n^2 qg \sqrt{p^2 + q^2}}{h^2} - gh \frac{\partial \zeta}{\partial y} + qf + \frac{\partial}{\rho \partial y} (h\tau_{yy}) + \frac{\partial}{\rho \partial x} (h\tau_{xy}) \tag{10}$$

Where, h is the water depth (m), p and q are the specific flow in the x and y directions ($m^2 s^{-1}$), ζ is the surface elevation (m), g is the acceleration due to gravity ($9.8 m s^{-2}$), n is the Manning’s coefficient, ρ is the water density ($1000 kg m^{-3}$), τ_{xx} , τ_{yy} , and τ_{xy} are the components of the effective shear stress along x and y directions ($N m^{-2}$), and f is the Coriolis (s^{-1}).

Two-dimensional (2D) mesh of size 100 m x 100 m was chosen to represent the downstream land. Comparison of different mesh sizes (100 m and 200 m) indicated no significant difference in model performance. The storage areas and downstream areas are connected using an inline structure (Budhigandaki dam) as shown in Fig. 3. “Storage Area” refers to upstream reservoir of the dam axis while “Downstream Study Area” represents the

Table 1 Data required for dam breach analysis of the Budhigandaki dam and mapping the downstream impacts

Data	Description	Source	Resolution/Remarks
DEM	Digital Elevation Model	SRTM <i>earthexplorer.usgs.gov</i> (Accessed: 10th Jan 2021)	1-Arc Second grids
Rainfall	Daily observed rainfall	Department of Hydrology and Meteorology (DHM), Nepal	13 stations; (1972–2014) 43 years data
Discharge	Mean Monthly observed streamflow	(BGHPP Development Committee 2014b)	1 station; (1964–2012) 49 years data
Land use	Land use/cover map	ICIMOD (2013) https://rds.icimod.org/Home/DataDetail?metadatald=9224 13th Jan 2021	30 m x 30 m grids
Manning’s Roughness Coefficient	Land use Roughness	Chow, 1959	Values
Infrastructure	Buildings, Roads, Bridges	Open Street Map (OSM) https://download.geofabrik.de/asia/nepal.html (Accessed: 20th Jan 2021)	Shapefiles

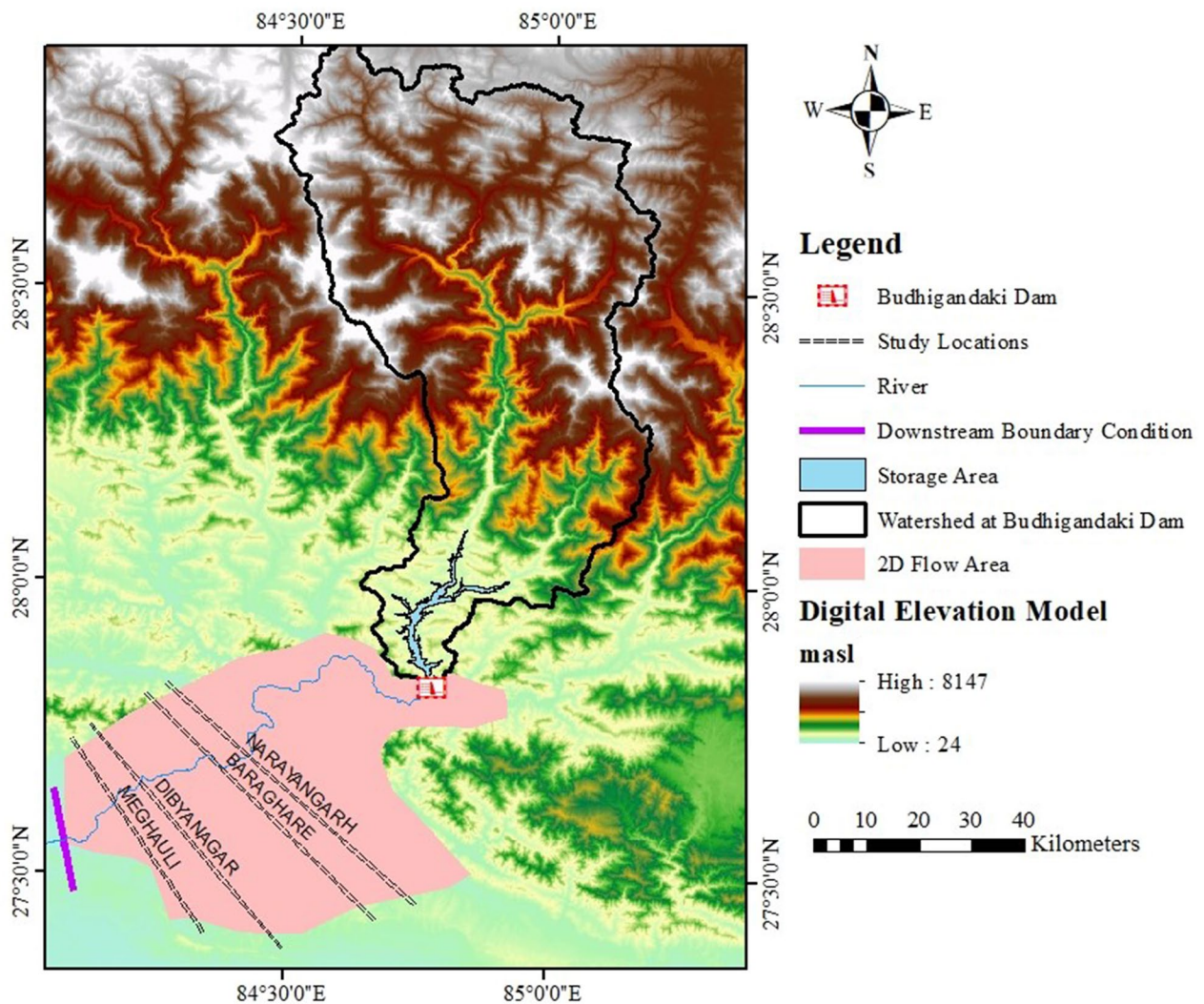


Fig. 3 HEC-RAS 2D flow area and model schematic for the flood simulation of Budhigandaki dam breach

four towns (Narayangarh, Baraghare, Divyanagar, and Meghauli) located downstream which are likely to be inundated in case of dam breach (BGHP, 2015). Boundary conditions are required at the upstream and downstream ends of the model for flood routing. The upstream boundary was fixed at the reservoir extent (storage area) and the boundary condition was provided in the form of flood hydrograph generated from PMF. Outlet is the downstream boundary past the settlement areas as shown in Fig. 3 while the boundary condition of normal depth is maintained by providing the river bed-slope obtained from the DEM.

Scenarios and sensitivity analysis

In order to quantify the downstream effects of the Budhigandaki dam breach, the following two scenarios have been simulated:

Scenario 1: Dam breach when reservoir is at FSL with PMF.

Scenario 2: Dam breach when reservoir is at FSL.

Only overtopping breach mode was analyzed as the dam is made up of concrete and there are less chances of other failure modes (Zhang et al. 2016). Moreover, for better understanding the Budhigandaki dam breach mechanism and impacts, sensitivity analysis of the following five important breach parameters as breach bottom elevation, breach bottom width, breach weir coefficient, breach formation time and breach side slope was carried out by varying their values over a reasonable range obtained from literature.

Scenario I have been considered as the base case. Sensitivity of the above-mentioned breach parameters on flood peak discharge, water surface elevation and flood

arrival time at the four downstream locations along with inundation area are analyzed considering the base case.

The inputs for the dam break analysis adopted for the base case i.e., Scenario I is listed in the Table 2. The values of breach parameters have been derived from FERC (1993), Office of the State Engineer (2020) and USACE (2014) specific for concrete dams.

Flood characteristics from 2D simulations

Using RAS Mapper, a series of flood maps were generated based on the outputs of the 2D simulation of the Scenario I dam breach. These maps were helpful in identifying the potentially risky and safe areas. The outputs of the HEC-RAS model were exported to GIS for further analysis and mapping.

Maximum Flood depth map Using the simulation results, flood inundation maps were prepared illustrating the maximum flood depths across the study area for the different scenarios.

Flood Hazard Vulnerability Map: A flood hazard vulnerability map based on the product of depth and velocity was prepared using the Australian Rainfall-Runoff Guidelines (Australian Rainfall and Runoff 2019) which categorize the flood in six zones as: *H1* ($D*V \leq 0.3$, $D_{max} = 0.3$ m, $V_{max} = 2.0$ m/s, safe for people, vehicles and buildings); *H2* ($D*V \leq 0.6$, $D_{max} = 0.5$ m, $V_{max} = 2.0$ m/s, unsafe for small vehicles); *H3* ($D*V \leq 0.6$, $D_{max} = 1.2$ m, $V_{max} = 2.0$ m/s, unsafe for vehicles, children and elderly); *H4* ($D*V \leq 1.0$, $D_{max} = 2.0$ m, $V_{max} = 2.0$ m/s, unsafe for people and vehicles); *H5* ($D*V \leq 4.0$, $D_{max} = 4.0$ m, $V_{max} = 4.0$ m/s, unsafe for people and vehicles, buildings vulnerable to structural damage) ; *H6* ($D*V > 4.0$, unsafe for people and vehicles, all buildings vulnerable to failure) where *D* and *V* refer to the flood depth and velocity, respectively while D_{max} and V_{max} refers to the maximum depth and maximum velocity, respectively.

Flood arrival Time Map Flood arrival time maps represent the computed time (in hours or days) from a specified time in the simulation when the water depth reaches a specified inundation depth. For the case of Budhigandaki dam breach, flood arrival times at the four settlement areas were calculated and mapped.

Results

Estimated values of PMP and PMF

The 1-day PMP value using the 13 precipitation stations was calculated to be 518 mm, 530 mm, 556 mm and 485 mm using Thiessen polygon, Kriging, inverse distance weighted (IDW), and Spline interpolation methods, respectively. As a worst-case scenario, we chose the IDW method, which gave the maximum value of PMP among the four methods, for generating the PMF hydrograph.

Table 2 Breach parameters for the base case of dam breach

Parameter	Value	Unit	Ranges for Sensitivity Analysis
Dam type	Double Curvature Concrete Arch		
Dam height	263	meters	
FSL	540	masl	
Breach mode	Overtopping		
Breach formation time	0.1	hours	0.05 h to 0.3 h
Breach width base	80	meters	55 m to 150 m
Breach weir coefficient	1.44		0.9 to 1.7
Side Slope	1.3H:1V		0.7H:1V to 2.5H:1V
Breach Bottom Elevation	450	masl	525masl to 450masl

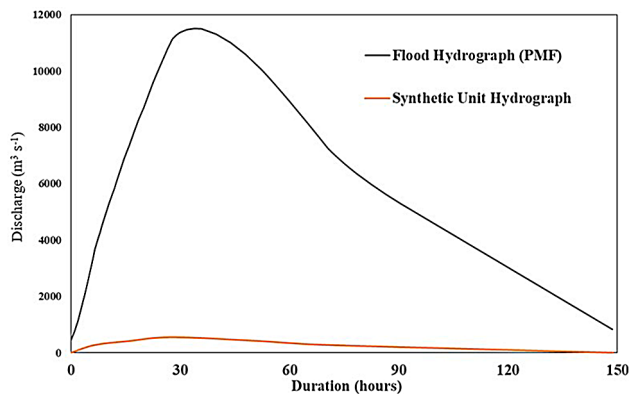


Fig. 4 Synthetic Unit Hydrograph and Probable Maximum Flood Hydrograph for the Budhigandaki dam

Using the input data listed in the Appendix 1, ordinates of the synthetic unit hydrograph was computed using Snyder’s method as shown in Fig. 4.

From the synthetic unit hydrograph and rainfall intensity duration curve, Direct Runoff Hydrograph was generated. The flood values are generated for a 60-minute interval by linear interpolation between the ordinates of the unit hydrograph. August is the month with the highest flows at the Budhigandaki dam site. Therefore, base flow of $441 \text{ m}^3 \text{ s}^{-1}$ which is the mean August flow (during 1964–2012) was added to obtain the final hydrographs (BGHPP Development Committee 2014b). The final results are plotted in Fig. 4. It can be seen that the peak discharge of $11,669 \text{ m}^3 \text{ s}^{-1}$ occurs at 33.9 h after the start of rainfall for PMF+base flow.

Flood depth and flood hazard vulnerability

The river valley of 110 km length from Budhigandaki dam to Megghauli was considered for the analysis. The maximum flood depth Fig. 5 shows that the flood depth is as high as 212 m in the upstream area as the river channel is narrow whereas the depth becomes lesser in the downstream river sections where the area is relatively wide and plain. The maximum water depths at Narayangarh is estimated to be 90 m followed by 50.3 m at Baraghare.

Similarly, Flood Hazard Vulnerability Map based on the depth and velocity was prepared as shown in Fig. 6. It can be identified from the map that all the downstream area lies in H6 zone i.e., unsafe for people and vehicles and all buildings are vulnerable to failure.

Flood arrival time

Simulated flood peak arrival times calculated at the four downstream settlement areas are shown in Fig. 7. It is useful in designing of early warning systems at these locations. It can be seen that the travel times range from 11.3 h (Narayangarh) to 17 h (Megghauli) immediately after the dam breach depending on the proximity from the dam.

Flood inundation across different land covers

As an impact of dam breach on land cover, it is seen that the inundated type to be most likely inundated is agricultural area (538 km^2). Similarly, 239 km^2 of forest is likely to be inundated second in rank. Grassland, water body, barren area, built-up area and shrub land are expected to be inundated with areas of 43 km^2 , 38

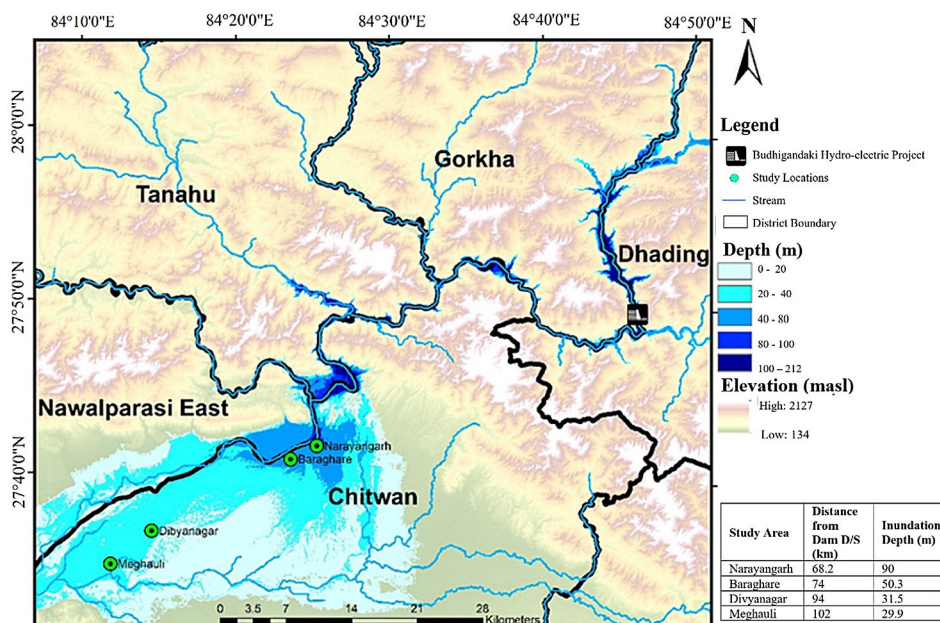


Fig. 5 Flood Inundation Map Based on Maximum Depths

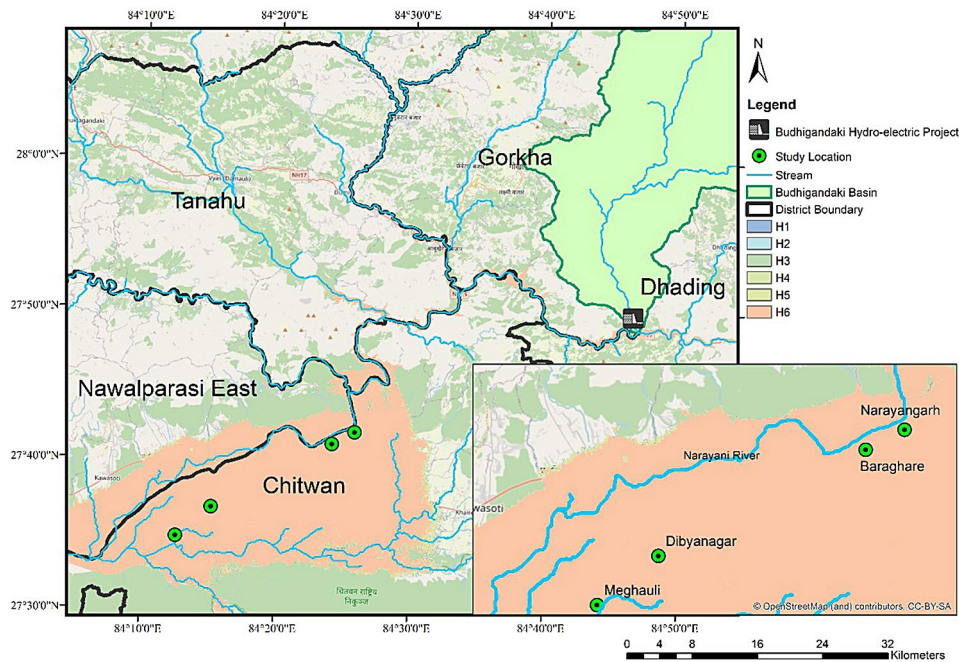


Fig. 6 Flood Hazard Vulnerability Mapping Based on Depth and Velocity

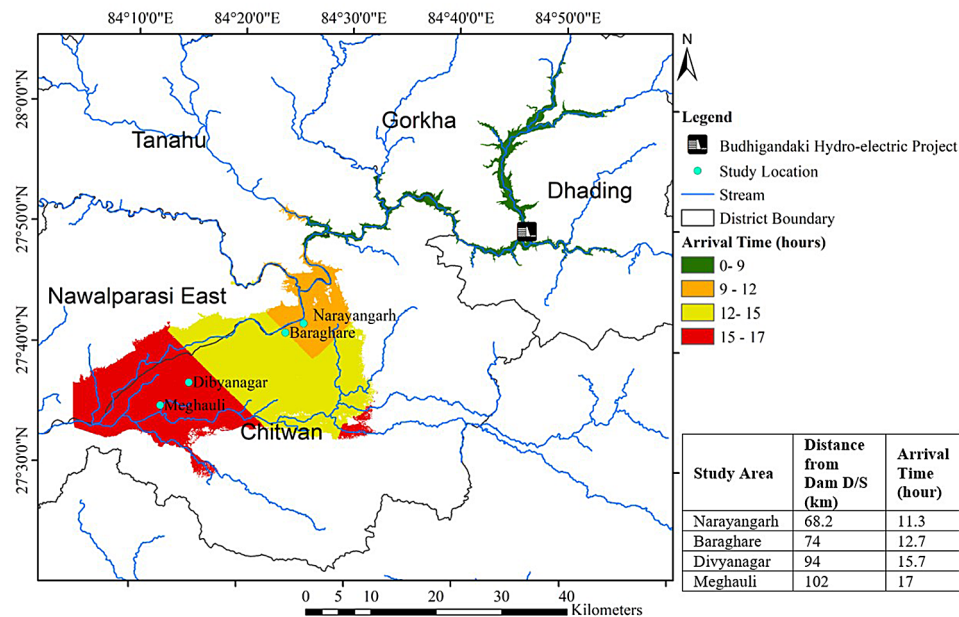


Fig. 7 Flood arrival time for the major downstream settlement locations; D/S is downstream

km², 25 km², 22 km² and 1.5 km² respectively as shown in Fig. 8.

Flood Impact on Water Surface Elevation (WSE) and peak discharge

Water surface elevations along the modelled river reach corresponding to the two scenarios are shown in Fig. 9. It is seen that the water surface is nearly 110 m above the bed level at immediate downstream

of the dam site while it is as low as 30 m in the downstream study areas. There is an enormous volume of water flowing down in a very short time because of the breach resulting in such high values of water depths along the river reach. There is very less change in the water surface elevation between Scenario-1 and 2. Also, at the settlement areas, the flow width is large i.e., flat plain area and hence lesser change is seen on the water surface elevation at downstream areas.

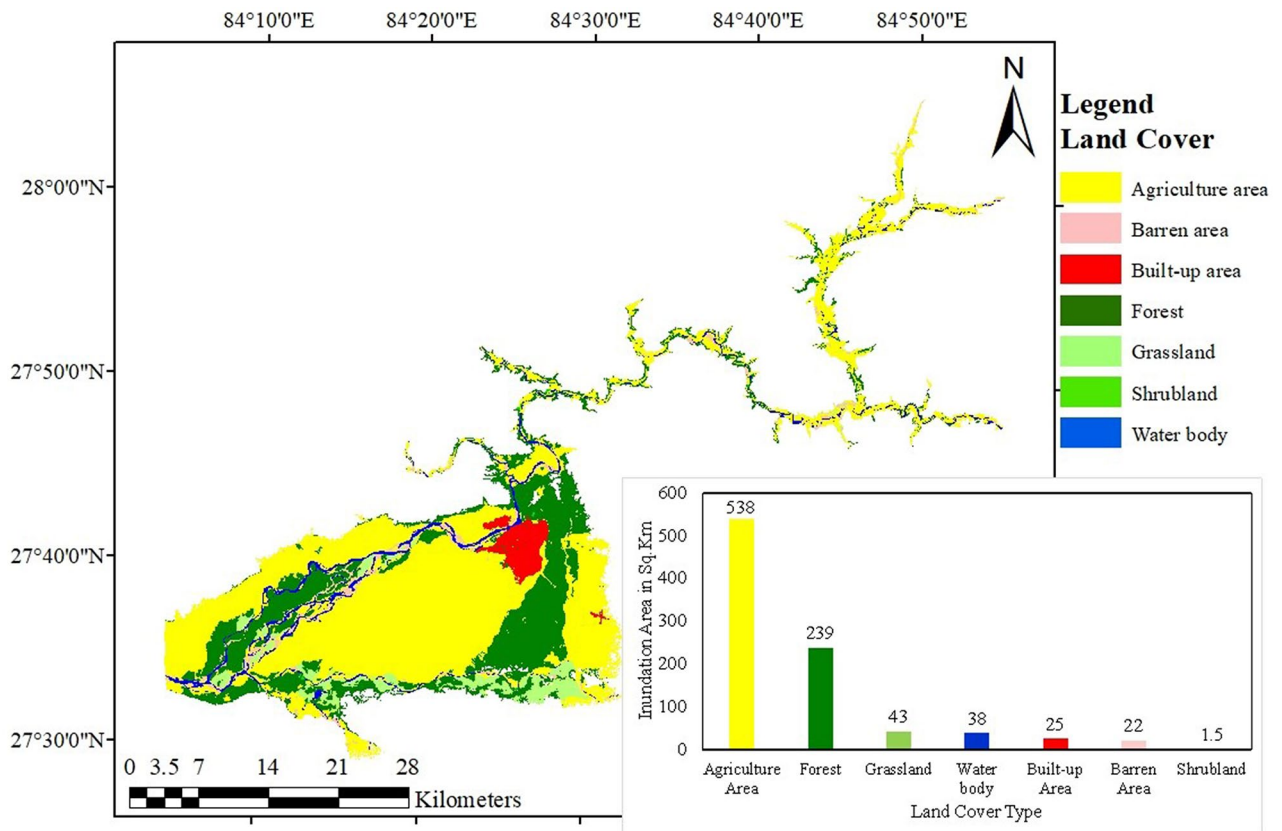


Fig. 8 Inundation extent due to dam breach by land cover

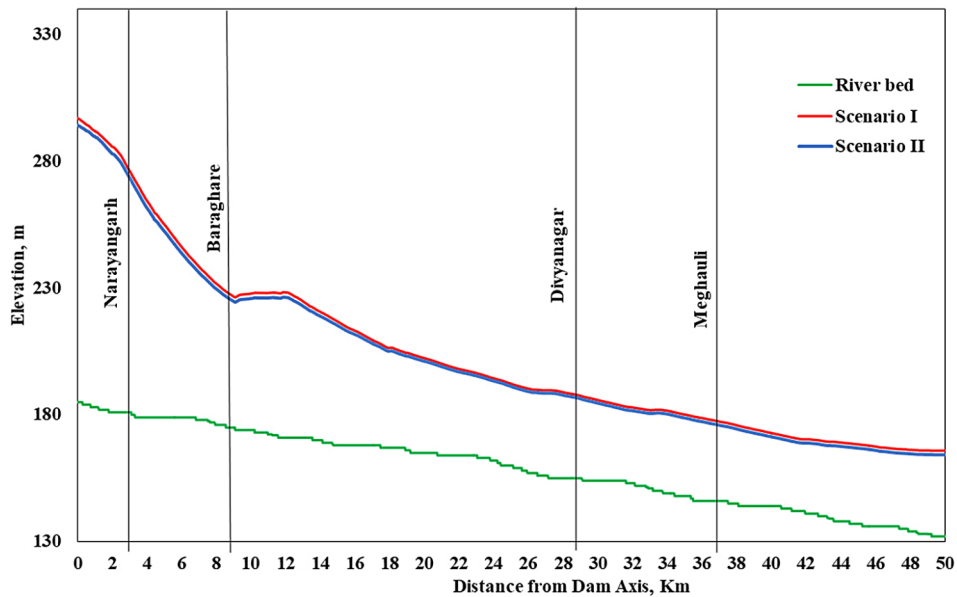


Fig. 9 Profile of water surface elevation and river bed for Scenario I and Scenario II. Scenario I: Dam Breach at FSL with PMF and Scenario II: Dam Breach at FSL without PMF

For the two scenarios (Scenario-1 and Scenario-2), the flow hydrographs have been compared at immediate downstream of the dam and at the four major settlement locations as shown in Fig. 10. It is to be noted that the peak discharge occurs nearly at the same time for both scenarios at all locations. At Narayangarh, peak discharges for Scenarios-1 and 2 are $511,587 \text{ m}^3 \text{ s}^{-1}$ and $501,479 \text{ m}^3 \text{ s}^{-1}$ respectively i.e., around 2% of difference in the value. Similarly, at Baraghare, the peak discharge for Scenario-1 is $454,267 \text{ m}^3 \text{ s}^{-1}$ whereas $441,862 \text{ m}^3 \text{ s}^{-1}$ for Scenario-2 and for Divyanagar, the peak discharge for Scenario-1 is $364,697 \text{ m}^3 \text{ s}^{-1}$ whereas $357,294 \text{ m}^3 \text{ s}^{-1}$ for Scenario II respectively. Lastly for Meghauli, the peak discharge for Scenario-1 is $294,928 \text{ m}^3 \text{ s}^{-1}$ whereas $286,813 \text{ m}^3 \text{ s}^{-1}$ for Scenario-2. It is obvious that the peak discharge for Scenario-1 is greater than that of Scenario-2, however, the differences in the peak values between the two scenarios are quite small (in the range of 2–3%). This implies that the storage volume of the dam is the major contributor to the flood discharge rather than the PMF.

Flood impact on infrastructure

The possible impact of inundation due to dam breach on buildings and roads was assessed. The total road

length includes several types of roads such as highways, feeder roads, district roads and local roads. The inundated highway road length has been computed separately and all other types of roads has been kept as other roads (Table 3). It can be seen that Chitwan is the most impacted district with 58.5% of buildings and 2,541 km of road likely to be inundated. Meanwhile, Gorkha is expected to be the least affected district with 2.6% buildings and 132.4 km road inundated. Also, 149,311 numbers of buildings are inundated in total. If the total number of persons on average per household is taken as 4.5 (Central Bureau of Statistics 2016), a total of about 0.7 million people are likely to be affected by inundation in the case of dam breach. This is about 2.3% of the total population of Nepal.

Sensitivity analysis

Sensitivity analysis was performed in order to estimate the impact of the breach parameters on the simulated floods in the downstream impacted areas. The values of the input breach parameters were changed within a reasonable range, one at a time, in the dam breach model and the corresponding values of the peak discharge, water surface elevation, flood arrival time

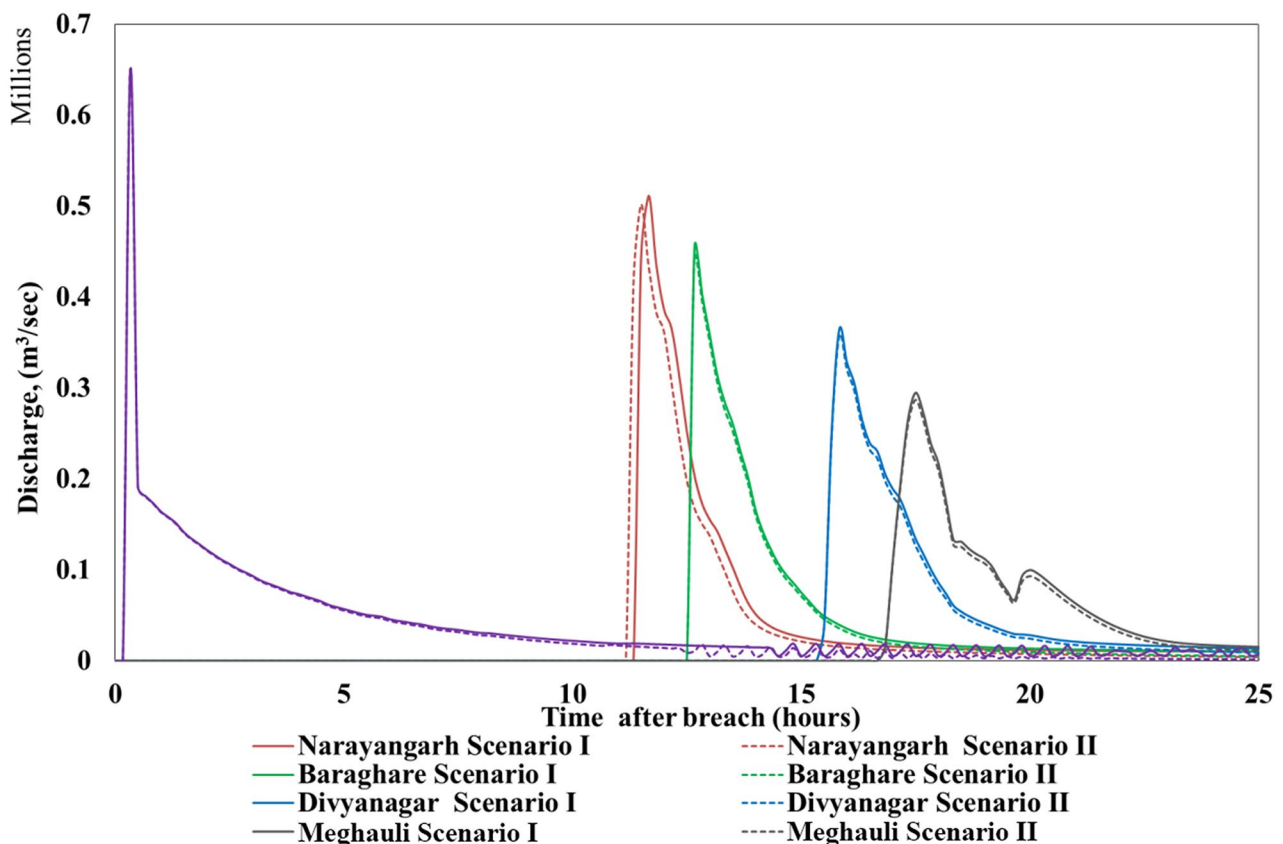


Fig. 10 Comparison of flood hydrographs at major study locations for Scenario I and Scenario II. Scenario I: Dam Breach at FSL with PMF and Scenario II: Dam Breach at FSL without PMF

Table 3 Impacts of inundation due to dam breach on infrastructure

Infrastructure	District				
	Chitwan	Dhading	Tanahu	Nawalparasi East	Gorkha
Buildings					
Total Number of Buildings	182,458	88,411	109,406	90,783	93,631
Number of Building Affected	106,739	2,370	3,614	34,242	2,346
Percentage Affected	58.5%	2.7%	3.30%	37.7%	2.5%
Road					
Total Highway Length (km)	1,377				
Total Highway Inundated (km)	88	33.1	7.4	25.6	
Total Other Road Length (km)	8,900				
Other Roads Inundated (km)	2,453.3	101.8	142.6	738.8	132.4
Total Road Length Inundated (km)	2,541.2	134.8	150.0	764.4	132.4

and land inundation area were recorded. Breach bottom elevation was varied from 450 masl to 525 masl. Similarly, breach width was varied from 55 m to 150 m and breach weir coefficient was varied from 0.9 to 1.7. Also, breach formation time was varied from 0.05 h to 0.3 h and breach side slope was varied from 0.7:1 to 2.5:1 ($H: V$). Results of the sensitivity analysis have been presented in Table 4.

Breach bottom elevation

It is seen from Table 4 that as the breach bottom elevation is increased from 450 masl to 525 masl, the value of peak discharge and WSE are significantly decreased at the different downstream locations. It is observed that a 30% increase in breach bottom elevation (450 masl to 475 masl) led to 20–35% decrease in peak discharge, 20–25% decrease in WSE at different downstream locations and nearly 30% decrease in inundation area (893 km² to 735 km²). However, the flood peak arrival time is not much altered due to change in breach bottom elevation.

Breach bottom Width

It is seen from Table 4 that an increase in breach width from 55 m to 150 m corresponds to an increase in discharge, WSE and inundation area but the change is not as significant as compared to that of change in breach bottom elevation. A 30% increase in breach width (80 m to 105 m) led to nearly 3% increase in peak discharge at all downstream locations. However, not much change is seen on the WSE, flood arrival time and inundation area due to change in breach bottom width.

Breach weir coefficient

An increase in the breach weir coefficient from 0.9 to 1.7 led to increase in discharge, WSE and inundation area but with a smaller magnitude compared to that of change in breach bottom elevation (Table 4). A 20% increase in breach weir coefficient (1.44 to 1.7) led to nearly 3%

increase in peak discharge at all downstream locations. Also, no significant change is seen on the WSE, flood arrival time and inundation area due to change in breach weir coefficient.

Breach formation time

Interestingly, there is very insignificant change in peak discharge, WSE, flood arrival time and inundation area due to varying breach formation time (Table 4). The values of peak discharge, WSE, flood arrival time and inundation area remain almost unchanged despite the breach formation time is increased up to 200% (0.1 h to 0.3 h).

Breach side slope

A 50% increase in the side slope (1.3:1 to 2:1) led to nearly 2–3% increase in peak discharge as shown in Table 4. Also, no significant change is seen on the WSE, flood arrival time and inundation area due to change in breach side slope.

Thus, results of the sensitivity analysis varying the values of the breach parameters, namely, dam breach bottom elevation, breach bottom width, breach weir coefficient, breach formation time and breach side slope on the peak discharge, WSE, flood arrival time and downstream inundation area has been summarized in Table 5. It can be seen that dam breach bottom elevation is the most sensitive parameter with respect to output values such as peak discharge, WSE and downstream inundation area while breach formation time is the least sensitive parameter with respect to all the output parameters.

Discussion

Input data

We have estimated the PMP followed by PMF which is the upstream boundary condition required for the dam breach model in HEC-RAS. The PMP value was chosen as 556 mm from the IDW method. Also, the PMP value as per the detail design report (BGHPP Development Committee 2014b) is 594 mm. Both the values of PMP are generated using Hershfield formula. However, this

Table 4 Sensitivity analysis of different breach parameters on peak discharge, water surface elevation, flood arrival time and land cover

Parameters	Breach Elevation (masl)			Breach Width (m)			Breach Weir Coefficient	Breach Formation Time (hour)			Breach Side Slope (H:V)									
	475	500	525	55 m	80 m	105 m		150 m	0.9	1.1	1.44	1.7	0.05	0.1	0.2	0.3	0.7:1	1.3:1	2:1	2.5:1
Peak discharge (m ³ s ⁻¹) (in 10 ⁴)	33.9	188	51.2	1.1	48.1	51.2	52.7	54.2	39.9	43.8	51.2	52.5	51.2	51.2	51.1	50.2	45.0	51.2	52.5	52.5
	33.4	150	45.4	1.1	42.8	45.4	46.8	49.0	40.4	43.0	45.4	46.7	45.5	45.4	45.4	45.7	43.3	45.4	46.7	46.7
	29.4	16.3	36.5	1.7	35.2	36.5	37.4	38.3	30.8	32.3	36.5	37.2	36.5	36.5	36.4	35.5	33.6	36.5	37.2	37.2
	22.8	13.6	29.5	1.1	28.3	29.5	30.3	31.1	26.2	27.4	29.5	30.1	29.5	29.5	29.5	29.4	28.3	29.5	30.1	30.1
Water surface elevation (masl)	266	243	271	198	269	271	273	275	266	268	271	273	271	271	271	271	269	271	273	274
	219	206	225	186	224	225	226	227	222	224	225	226	225	225	225	225	224	225	227	228
	184	178	187	161	186	187	187	187	185	186	187	187	186	186	186	186	186	187	189	191
	172	166	176	153	175	176	176	177	174	175	176	176	176	176	176	176	175	176	179	181
Flood arrival time (hours)	11.3	11.3	11.3	11.3	11.3	11.3	11.3	11.3	11.5	11.5	11.5	11.5	11.3	11.3	11.3	11.3	11.3	11.3	11.3	11.3
	12.7	12.7	12.7	12.7	12.7	12.7	12.7	12.7	12.7	12.7	12.7	12.7	12.5	12.5	12.5	12.5	12.5	12.5	12.5	12.5
	15.8	16.0	15.67	15.7	15.7	15.7	15.7	15.7	15.7	15.7	15.7	15.7	15.6	15.6	15.6	15.6	15.6	15.6	15.6	15.6
	17.2	17.5	17.0	17.0	17.2	17.0	17.0	17.0	17.2	17.2	17.0	17.0	17.0	17.0	17.0	17.0	17.1	17.0	17.0	17.1
Land cover	735	539	893	220	881	893	903	915	859	877	893	902	893	893	892	891	880	893	903	903
	455	351	527	137	521	527	533	533	510	519	527	532	527	527	527	526	521	527	533	533
	24.6	23.6	25.3	3.61	25.2	25.3	25.3	25.3	25.1	25.2	25.3	25.3	25.3	25.3	25.3	25.2	25.3	25.3	25.3	25.3

slight variation in the PMP values is due to the difference in the values of frequency factor. The value of frequency factor in this study is taken as 15 (Hershfield 1965). Subsequently, the PMF value for this study is generated using Snyder's Unit Hydrograph Method with peak discharge as 11,669 m³ s⁻¹. Besides, by using regional method the PMF was calculated to be 11,479 m³ s⁻¹ and regional regression flood analysis method 11,957 m³ s⁻¹ (Department of Electricity Development 2006). Hence, the PMF values considered in this study are assumed to be reliable.

Impacts of dam breach and sensitivity analysis of dam breach parameters

Simulation results of Scenario I and Scenario II showed that there is a huge peak discharge immediately downstream of the dam breach (Fig. 10 and the difference in discharge values for both scenarios is low. The reason for this is due to the large storage volume of the dam leading to minimum effect of PMF being observed. Also, the downstream tributaries are much smaller compared to the Budhigandaki mainstream river. Hence, their additional impacts on the dam breach flood magnitudes can be considered to be marginal. Additionally, the outputs such as peak discharge, WSE, flood arrival time and inundation area from the dam breach has been estimated as a standalone event. The impact of addition of inflows from the other tributaries (for example, due to localized cloudburst events) to the mainstream river in the downstream settlement area could be areas of further study.

Previous dam breach analysis on Budhigandaki dam has been carried out by Tractebel and jade consult as JV using TELEMAC software (BGHPP Development Committee 2014a). The output results of the previous study appeared to be quite different from the study carried out using HEC-RAS. There could be various reasons for such discrepancies. The TELEMAC model has considered full dam breach whereas our study does not consider full dam breach. Also, the earlier model has considered high accuracy resolution LiDAR data and other input data (mesh size 30 m*50 m) whereas our study considers 30 m*30 m DEM data and 100 m*100 m mesh size due to model stability issues. However, the pattern of change in peak discharge and WSE at the different study locations are quite similar for both models.

Dam breach analysis has been carried out in different parts of the world using HEC-RAS adopting a methodology similar to ours. For example, simulations of the breach of Batutegi earthen Dam, Indonesia (Wahyudi 2004), Mosul earthen Dam, Iraq (Basheer et al. 2017) and the results of sensitivity analysis are found out to be quite similar to this study. All these studies showed that dam breach bottom elevation is the most sensitive parameter. Further, the trends in WSE and peak discharge with time and distance from the dam obtained in these studies

Table 5 Summary of Sensitivity Analysis

Parameter	Sensitivity on Peak discharge	Sensitivity on WSE	Sensitivity on Flood arrival time	Sensitivity on Downstream inundation area
Dam Breach Bottom Elevation	High	High	Low	High
Dam Breach Bottom Width	Moderate	Low	Low	Moderate
Weir Coefficient Values	Moderate	Low	Low	Moderate
Breach Formation Time	Low	Low	Low	Low
Breach Side Slope	Moderate	Low	Low	Moderate

are also comparable to those of our study. The WSE and peak discharge increased with the increase in the breach parameters as breach bottom elevation, breach bottom width, breach weir coefficient and breach side slope. The peak discharge decreased with increase in breach formation time and negligible change was seen on WSE. Hence, through sensitivity analysis, it is seen that dam breach bottom elevation is the most sensitive parameter while breach formation time is the least sensitive parameter with regards to the floods.

Challenges to flood management

This analysis of a hypothetical dam breach provides insight to the level of possible damage should such a breach occur. Also, it can be deduced from this study that construction of embankments along the river is not a practical mitigation measure because of the extremely high-water depths (nearly 90 m) that these structures need to retain within them. Hence, other non-structural preventive measures such as creating awareness regarding flood risks, community-based flood early warning system (CBFEWS), training and deployment of efficient disaster response teams, zoning of high-risk areas, avoiding construction/settlements in such areas, identification of evacuation centers etc. are recommended. The Yokohama Strategy and Plan of Action (World Conference on Natural Disaster Reduction 1994), Hyogo Framework for Action 2005–2015 (International Strategy for Disaster Reduction 2005), and the current Sendai Framework for Action 2015–2030 (United Nations 2015) highlight the importance of early warning in reducing disaster risk and enhancing the resilience of vulnerable communities. CBFEWS generates and disseminates meaningful and timely flood warnings to vulnerable communities threatened by flood, so they can prepare and act correctly in sufficient time to minimize the possibility of harm. Owing to non-structural measures, the response and adaptation to floods of the vulnerable communities vary widely and are impacted upon by various factors, such as community resilience and susceptibility to flood. Also, the effectiveness of the non-structural measures appears sensitive to the socio-economic changes and governance arrangements (Dawson et al. 2011). Nonetheless, non-structural measures provide flexible flood management

options for adapting to the ever-changing river basins, socio-economic and climate scenarios, and are in line with the spirit of environment friendly and sustainable development (Shah et al. 2018). Also, research on identification of shelter areas and evacuation plan can be an extension of this study using network analysis, buffers and proximity analysis in GIS. Moreover, the sensitivity analysis depicts the most sensitive breach parameters which need to be considered with extreme importance during planning, design, construction and operation of the dam.

Conclusions

This paper simulated the dam breach scenarios of the proposed Budhigandaki dam in central Nepal using HEC-RAS and assessed the impacts on the downstream settlements. Flood peaks, water surface elevations and flood arrival times were calculated for the two scenarios with and without PMF. In addition, sensitivity analysis was carried out to examine the influence of the breach parameters on the flood characteristics.

Results show that the entire downstream area lies in high hazard zone with flood arrival times at Narayangarh, Baraghare, Divyanagar and Meghauli ranges from 11.3 h to 17 h. Moreover, a total of 1,49,311 number of buildings are prone to inundation in the case of dam breach along with 671,900 lives at risk and around 3,500 km stretch of road most likely to be severely damaged. The dam-break flood peak exceeds $650,000 \text{ m}^3\text{s}^{-1}$ in the immediate downstream of the dam while it attenuates to 511,000 and $286,000 \text{ m}^3\text{s}^{-1}$ at Narayangarh and Meghauli, respectively. The maximum depth of water ranges from 30 m (in the downstream flat areas) to 212 m (in the upstream steep gorges) clearly discarding the physical and economic feasibility of structural measures for flood management in this case. In addition, 538 km^2 of agricultural land and 25 km^2 of built-up land is at risk of flood inundation. Therefore, it is imperative to implement preventive and non-structural measures such as creating awareness regarding flood risks, developing community-based flood early warning system (CBFEWS), training and deployment of efficient disaster response teams, zoning of high-risk areas, avoiding construction/settlements in such areas, identification of evacuation centers, monitoring

and constant auscultation of the structure and developing robust and efficient emergency and alert plans.

Furthermore, the differences in the peak discharges and water surface elevations between the two scenarios are very less at the study locations. This implies that the impact of the huge storage volume of the reservoir on the breach flood characteristics is considerably larger in comparison to the PMF. In addition, change in dam breach bottom elevation was found to be the most sensitive to floods compared to other dam breach parameters.

Additionally, the methodology applied in this study is conveniently replicable of other dams, large or small. However, the simulation run-times may vary depending upon the size of the dam, mesh size, simulation time step and other model complexities. It is to be noted that the case may change for snow fed rivers and glacier lakes. Also, while applying this method to other projects, one should always be careful about the boundary conditions and the initial values of dam breach parameters as they vary depending upon the dam under consideration.

Nepal has currently only one storage dam hydropower project (Kulekhani) in operation. With a greater number of storage projects being planned and under construction, this study could be a useful reference for such future projects. Moreover, this study provides interesting results particularly related to the sensitivity of the breach parameters of concrete arch dams, which could be applicable in study of similar dams in other regions of the world.

Abbreviations

A	Catchment Area (km ²)
C _p	Peak flow coefficient (-)
C _t	Lag Coefficient (-)
f	Coriolis (s ⁻¹)
g	acceleration due to gravity (m s ⁻²)
h	water depth (m)
K	Frequency Factor (-)
L	main channel length from basin outlet to upstream watershed boundary (km)
L _{ca}	main channel length from outlet to a point nearest to centroid of watershed (km)
M	Mean of Maximum daily rainfall (mm)
n	Manning's Coefficient (-)
p	Specific flow in x-direction (m ² s ⁻¹)
PMP	Probable maximum precipitation (mm)
Q	Discharge (m ³ s ⁻¹)
q	Specific flow in y-direction (m ² s ⁻¹)
q _p	Unit peak discharge (m ³ s ⁻¹)
S	Standard Deviation (mm)
T _b	Base time (hours)
T _d	Rainfall excess duration time (hours)
T _{lag}	Basin Lag time (hours)
W ₅₀	Width of unit hydrograph at discharge value exceeded 50% of the peak discharge (hours)
W ₇₅	Width of unit hydrograph at discharge value exceeded 75% of the peak discharge (hours)
ζ	Surface Elevation (m)
ρ	Water Density (kg m ⁻³)
τ	Effective Shear Stress (N m ⁻²)
τ _{xx}	Effective Shear Stress along x direction (N m ⁻²)
τ _{xy}	Effective Shear Stress along x and y direction (N m ⁻²)
τ _{yy}	Effective Shear Stress along y direction (N m ⁻²)

Acknowledgements

We wish to express my very deepest thanks and gratitude to Mr. Shreeram Shrestha, Civil Engineer, Chilime Hydropower Company Limited, Nepal for his continuous guidance, inspiration and encouragement during the initial preparation of building HEC-RAS model to result interpretation and completion of this study.

Author contributions

A.A. and P.K.B. devised the project, the main conceptual ideas, and the proof outline. A.A. worked out almost all of the technical details, prepared figures, and performed the model analysis for the suggested topics. A.A., P.K.B. and U.B. verified the numerical results. A.A. and V.P.P. interpreted the Results. A.A. with the help of U.B., P.K.B., and V.P.P. wrote the manuscript. U.B., P.K.B., and V.P.P. worked on the discussion of results and commented on the manuscript. A.A. finalizes the manuscript after all the edits.

Funding

This research received no specific grant from any funding agency in the public, commercial, or not-for-profit sectors.

Data availability

No datasets were generated or analysed during the current study.

Declarations

Competing interests

The authors declare no competing interests.

Received: 31 March 2024 / Accepted: 16 July 2024

Published online: 01 September 2024

References

- American Geophysical Union (1938) *Reports and Papers, Hydrology*
- Aureli F, Maranzoni A, Petaccia G (2021) Review of historical dam-break events and laboratory tests on real topography for the validation of numerical models. *Water* 13(14). <https://doi.org/10.3390/w13141968>
- Australian Rainfall and Runoff (2019) *A Guide to Flood Estimation, Book 6 - Flood Hydraulics*
- Basheer TA, Wayayok A, Yusuf B, Rowshon MK, Basheer TA, Kamal R (2017) Dam breach parameters and their influence on flood hydrographs for Mosul dam. *Article J Eng Sci Technol* 12(11):2896–2908. <https://www.researchgate.net/publication/328475986>
- BGHPP Development Committee (2014a) *Feasibility Study And Detailed Design of Budhi Gandaki HPP, Vol. 2B: Assessment of Downstream Impacts*
- BGHPP Development Committee (2014b) *Feasibility Study and Detailed Design of Budhigandaki HPP Vol. 2A: Hydrological and Meteorological Analysis*
- Bricker JD, Schwanghart W, Adhikari BR, Moriguchi S, Roeber V, Giri S (2017) Performance of models for Flash Flood warning and Hazard Assessment: the 2015 Kali Gandaki Landslide Dam Breach in Nepal. *Mt Res Dev* 37(1):5–15. <https://doi.org/10.1659/MRD-JOURNAL-D-16-00043.1>
- C Froehlich D (1995) Embankment dam breach parameters revisited. *Int Water Resour Eng Conf - Proc* 1(January 1995):887–891
- Cental Bureau of Statistics (2016) *Statistical Pocket Book of Nepal*. www.cbs.gov.np
- Dawson RJ, Ball T, Werritty J, Werritty A, Hall JW, Roche N (2011) Assessing the effectiveness of non-structural flood management measures in the Thames Estuary under conditions of socio-economic and environmental change. *Glob Environ Change* 21(2):628–646. <https://doi.org/10.1016/j.gloenvcha.2011.01.013>
- Department of Electricity Development (2006) *Design Guidelines for Head-works of Hydropower Projects*. <https://www.doed.gov.np/pages/guidelines-and-manuals>
- Dincergok T (2007) The role of dam safety in dam-break induced flood management. *International Conference on River Basin Management*, 683–691
- Ettema R, Baker ME, Teal M, Trojanowski J (2021) Ice-Run Destruction of Spencer Dam on Nebraska's Niobrara River. *CGU HS Committee on River Ice Processes and the Environment, 21st Workshop on the Hydraulics of Ice-Covered Rivers, Saskatoon, Saskatchewan, Canada*

- Fang CH, Chen J, Duan YH, Xiao K (2017) A new method to quantify breach sizes for the flood risk management of concrete arch dams. *J Flood Risk Manag* 10(4):511–521. <https://doi.org/10.1111/jfr3.12240>
- Federal Energy Regulatory Commission (FERC) (1993) *FERC Engineering Guidelines*
- FERC (2001) *FERC Engineering Guidelines for the Evaluation of Hydropower Projects*
- Government of Nepal (2020) *The Fifteenth Plan (Fiscal Year 2019/20–2023/24)*. www.npc.gov.np
- Gyawali DR, Devkota LP (2015) Dam Break Analysis using HEC-RAS: A Case Study of Proposed Koshi High Dam. *Proceedings of the Seminar on Water and Sustainable Development*
- Hershfield DM (1965) Method for estimating probable Maximum Precipitation. *J Am Waterworks Association* 57:965–972
- Independent Forensic Team (2022) *Final Investigation of Failures of Edenville and Sanford Dams*
- International Strategy for Disaster Reduction (2005) Hyogo framework for action 2005–2015. *World Conference on Disaster Reduction, January 2005*, 508–516. https://doi.org/10.1007/978-1-4020-4399-4_180
- Lempérière F (2017) Dams and floods. *Elsevier* 3(1):144–149. <https://doi.org/10.1016/J.ENG.2017.01.018>
- Leng Q, Zhang M, Zhao G, Mao S, Jiang A (2023) Simulation and Hazard Map of flooding caused by the Break of a concrete gravitational dam. *Lecture Notes Civil Eng* 264 LNCE:1248–1260. https://doi.org/10.1007/978-981-19-6138-0_109
- Nepal Electricity Authority (2022) *Nepal Electricity Authority, A Year in Review- Fiscal Year 2021/2022*. www.nea.org.np
- Office of the State Engineer (2020) *Guidelines for Dam Breach Analysis*
- Pandey BR, Knoblauch H, Zenz G (2023) Potential dam Breach Flood Hazard Assessment of Kulekhani Reservoir Rock fill dam using 2D diffusion and full dynamic shallow water equation defining Coriolis Effect. *Preprints Org*. <https://doi.org/10.20944/preprints202311.0088.v1>
- Shah MAR, Rahman A, Chowdhury SH (2018) Challenges for achieving sustainable flood risk management. *J Flood Risk Manag* 11:S352–S358. <https://doi.org/10.1111/jfr3.12211>
- Shugar DH, Jacquemart M, Shean D, Bhushan S, Upadhyay K, Sattar A, Schwanghart W, McBride S, van Wyk de Vries M, Mergili M, Emmer A, Deschamps-Berger C, McDonnell M, Bhambri R, Allen S, Berthier E, Carivick JL, Clague JJ, Dokukin M, Westoby MJ (2021) A massive rock and ice avalanche caused the 2021 disaster at Chamoli. *Indian Himalaya Sci* 373(6552):300–306. <https://doi.org/10.1126/science.abh4455>
- Singh KP, Snorrason A (1984) Sensitivity of outflow peaks and flood stages to the selection of dam breach parameters and simulation models. *J Hydrol* 68(1–4):295–310. [https://doi.org/10.1016/0022-1694\(84\)90217-8](https://doi.org/10.1016/0022-1694(84)90217-8)
- United Nations (2015) Sendai Framework for Disaster Risk Reduction. In *UN World Conference*
- United States Department of Interior (1988) Downstream Hazard Classification Guidelines. In *ACER Technical Memorandum No. 11, Assistant Commissioner - Engineering and Research, Denver, Colorado*
- USACE (2014) *Using HEC-RAS for Dam Break Studies*. www.hec.usace.army.mil
- USACE (2018) *Hydrologic Engineering Requirements for Reservoirs Engineer Manual*
- USACE (2024) *HEC-RAS River Analysis System HEC-RAS Hydraulic Reference Manual*
- Vincent E, Emeka OM, Dominic P (2020) Dam and its Failure: A Brief Review of some selected Dams around the World. *Adamawa State University Journal of Scientific Research*, 8. <http://www.adsujsr.com>
- Wahyudi E (2004) *Dam Break Analysis; A Case Study*
- World Conference on Natural Disaster Reduction (1994) Yokohama Strategy and Plan of Action for a Safer World: Guidelines for Natural Disaster Prevention, Preparedness and Mitigation. *World Conference on Natural Disaster Reduction Yokohama, Japan, 23–27 May 1994, May 1994*, 23–27
- World Meteorological Organization (2009) *Manual on estimation of probable maximum precipitation (PMP)*
- Zhang L, Peng M, Chang D, Xu Y (2016) Statistical Analysis of Failures of Concrete Dams. In *Dam Failure Mechanisms and Risk Assessment*. <https://doi.org/10.1002/9781118558522.ch4>

Publisher's Note

Springer Nature remains neutral with regard to jurisdictional claims in published maps and institutional affiliations.